Journal of Visualized Experiments

Decellularization of Whole Human Heart inside a Pressurized Pouch in an Inverted Orientation

--Manuscript Draft--

Article Type:	Methods Article - JoVE Produced Video
Manuscript Number:	JoVE58123R2
Full Title:	Decellularization of Whole Human Heart inside a Pressurized Pouch in an Inverted Orientation
Keywords:	Pressure head; pericardium; Decellularization; turbidity; human heart; flow dynamics.
Corresponding Author:	Doris Taylor Texas Heart Institute Houston, UNITED STATES
Corresponding Author's Institution:	Texas Heart Institute
Corresponding Author E-Mail:	DTaylor@texasheart.org
Order of Authors:	Doris A. Taylor
	Luiz C. Sampaio
	Rafael Cabello
	Abdelmotagaly Elgalad
	Rohan Parikh
	R Patrick Wood
	Kevin A. Myer
	Alvin Yeh
	Po-Feng Lee
Additional Information:	
Question	**Response**
Please indicate whether this article will be Standard Access or Open Access.	Standard Access (US$2,400)
Please indicate the **city, state/province, and country** where this article will be **filmed**. Please do not use abbreviations.	Regenerative Medicine Research Laboratory, 9th Floor, texas heart Institute, 6770 Bertner Ave., Houston, TX 77030

TITLE:

Decellularization of Whole Human Heart inside a Pressurized Pouch in an Inverted Orientation

AUTHORS:

Doris A. Taylor[1], Luiz C. Sampaio[1], Rafael Cabello[1], Abdelmotagaly Elgalad[1], Rohan Parikh[1], R Patrick Wood[2], Kevin A. Myer, MSHA[2], Alvin T. Yeh[3], Po-Feng Lee[1]

[1]Regenerative Medicine Research, Texas Heart Institute, Houston, TX, USA
[2]Lifegift Organ Donation Center, Houston, TX, USA
[3]Biomedical Engineering, Texas A&M University, College Station, TX, USA

CORRESPONDING AUTHOR:

Doris A. Taylor (dtaylor@texasheart.org)

EMAIL ADDRESSES OF CO-AUTHORS:

Luiz C. Sampaio (lsampaio@texasheart.org)
Rafael Cabello (Rafael.Cabello@my.unthsc.edu)
Abdelmotagaly Elgalad (aelgalad@texasheart.org)
Rohan Parikh (rmr@texasheart.org)
R Patrick Wood (rpwood@lifegift.org)
Kevin A. Myer, MSHA (kmyer@lifegift.org)
Alvin T. Yeh (ayeh@tamu.edu)
Po-Feng Lee (plee@texasheart.org)

KEYWORDS:

Pressure head, pericardium, decellularization, turbidity, human heart, flow dynamics

SUMMARY:

This method enables decellularization of a complex solid organ using a simple protocol based on osmotic shock and perfusion of ionic detergent with minimal organ matrix disruption. It comprises a novel decellularization technique for human hearts inside a pressurized pouch with real-time monitoring of flow dynamics and cellular debris outflow.

ABSTRACT:

The ultimate solution for patients with end-stage heart failure is organ transplant. But donor hearts are limited, immunosuppression is required, and ultimately rejection can occur. Creating a functional, autologous bio-artificial heart could solve these challenges. Biofabrication of a heart comprised of scaffold and cells is one option. A natural scaffold with tissue-specific composition as well as micro- and macro-architecture can be obtained by decellularizing hearts from humans or large animals such as pigs. Decellularization involves washing out cellular debris while preserving 3D extracellular matrix and vasculature and allowing "cellularization" at a later timepoint. Capitalizing on our novel finding that perfusion decellularization of complex organs is possible, we developed a more "physiological" method to decellularize non-transplantable human hearts by placing them inside a pressurized pouch, in an inverted orientation, under

controlled pressure. The purpose of using a pressurized pouch is to create pressure gradients across the aortic valve to keep it closed and improve myocardial perfusion. Simultaneous assessment of flow dynamics and cellular debris removal during decellularization allowed us to monitor both fluid inflow and debris outflow, thereby generating a scaffold that can be used either for simple cardiac repair (*e.g.* as a patch or valve scaffold) or as a whole-organ scaffold.

INTRODUCTION:

Heart failure leads to high mortality in patients. The ultimate treatment option for end-stage heart failure is allo-transplantation. However, there is a long wait-list for transplantation due to the shortage of donor organs, and patients face post-transplantation hurdles that range from life-long immunosuppression to chronic organ rejection[1,2]. Bioengineering functional hearts by repopulating decellularized human-sized hearts with a patient's own cells could circumvent these hurdles[3].

A major step in "engineering" a heart is the creation of a scaffold with appropriate vascular and parenchymal structure, composition and function to guide the alignment and organization of delivered cells. In the presence of the appropriate framework, cells seeded on the scaffold should recognize the environment and perform the expected function as part of that organ. In our opinion, decellularized organ extracellular matrix (dECM) comprises the necessary characteristics of the ideal scaffold.

By utilizing intrinsic vasculature, complex whole-organ decellularization can be achieved via antegrade or retrograde perfusion[4] to remove cellular components while preserving the delicate 3D extracellular matrix and vasculature[2,5-7]. A functional vasculature is important in bioengineering whole organs just as it is *in vivo*, for nutrient distribution and waste removal[8]. Coronary perfusion decellularization has been proven to be effective in creating decellularized hearts from rats[4], or pigs[4,7,9-13], and humans[5,7,14-16]. Yet, integrity of the valves, atria and other "thin" regions can suffer.

Human-size decellularized heart scaffolds can be obtained from pigs using pressure control[7,9-12] or infusion flow rate control[13,17] and from human donors using pressure control[5,7,14,15]. Decellularization of human donor hearts occurs over 4-8 days under pressure controlled at 80-100 mmHg in upright orientation[5,15,16] or over 16 days under pressure controlled at 60 mmHg [,14]. Under antegrade, pressure-controlled decellularization, the aortic valve competency plays a crucial role in maintaining coronary perfusion efficiency and stable pressure at the aortic root. Our previous work revealed that the orientation of the heart influences its coronary perfusion efficiency during the decellularization procedure and therefore the scaffold integrity in the end[9]. As a continuation of our previous work[9], we introduce a novel concept wherein a pericardium-like pouch is added to improve whole-heart decellularization. We describe the decellularization of human hearts placed inside pressurized pouches, inversely oriented, and under pressure controlled at 120 mmHg at the aortic root. This protocol includes monitoring the flow profile and collection of outflow media throughout the decellularization procedure to evaluate coronary perfusion efficiency and cell debris removal. Biochemical assays are then performed to test the effectiveness of the method.

PROTOCOL:

All experiments adhered to the ethics committee guidelines from the Texas Heart Institute.

1. Organ Preparation

Note: In collaboration with LifeGift, a nonprofit organ procurement organization in Texas (http://www.lifegift.org), donated human hearts not suitable for transplant were used for research with approved consent.

1.1. To procure hearts, intravenously infuse 30,000 U heparin to the hearts. Securely suture cardioplegia cannula in the aorta and attach a clamped perfusion line. Perforate the inferior vena cava (IVC) to vent the right heart. Cut either the left superior pulmonary vein or the left atrial appendage to vent the left chambers of the heart.

1.2. Infuse 1 L of cardioplegia or heparinized saline. Dissect aortic arch branches, superior vena cava (SVC) and other pulmonary veins to release the heart from any vascular or surrounding tissue attachment. Submerge the well-heparinized heart in iced saline solution.

1.3. Inspect the donated human heart (both anteriorly and posteriorly, **Figure 1**). Place the heart on a dissecting tray and inspect for any structural damage or anatomical malformations. If liver and/or lungs were procured for transplantation, the heart may present with a short inferior vena cava and/or absence of left atrial posterior wall.

1.4. Perform internal inspection for possible defects – atrial septal defect (ASD), ventricular septal defect (VSD), or valve (aortic, pulmonary, mitral, tricuspid) malformation.

1.5. If a septal defect is present, correct it with appropriate sutures (**Figure 2A**, **2B**). The correction of septal defects is needed to monitor decellularization progress via pulmonary artery (PA) outflow turbidity measurement. Correction of the septal defect removes left to right shunt, hence, the outflow from PA represents the outflow from the coronary circulation through the coronary sinus.

1.6. Ligate superior and inferior vena cava with 2-0 silk suture (**Figure 2C**).

1.7. Dissect the aorta (Ao) away from the main PA (**Figure 2D**) for subsequent cannulation.

1.8. Insert connectors, based on the diameter of the vessel, (**Figure 3**) into Ao and PA and secure them with 2-0 silk sutures (**Figure 4A**).

1.9. Insert a tubing line through the left atrium (**Figure 4B**) and toward the left ventricle (LV) (**Figure 3**), using one of the pulmonary vein orifices.

1.10. Connect an infusion line to the connector placed in the Ao and the outflow line to the one in the PA (**Figure 3**).

1.11. Place the prepared heart into a polyester pouch in inverted orientation (upside down).

1.12. Place the pouch with heart into a perfusion container and close the lid (**Figure 4C**).

1.13. Connect each of the lines to the respective ports in the rubber stopper (based on the diameter of container) and insert it to the lid of the perfusion container to seal the polyester pouch (**Figure 4C** and **Figure 5B**).

1.14. Perfuse 1x phosphate buffered saline (PBS) (136 mM NaCl, 2.7 mM KCl, 10 mM Na_2HPO_4 and 1.8 mM KH_2PO_4 in distilled water, pH 7.4) via the infusion port of the rubber stopper to verify outflow from the PA and from the line inserted into LV.

1.15. Use this flow to clean the organ of any residual traces of blood in the vasculature. If flow is not observed, tighten the connection lines as they might be loose.

2. System Setup and Organ Decellularization Procedure

2.1. Assemble the bioreactor and place in an upright orientation (**Figure 5**). The perfusion system includes a personal computer (PC), proportional-integral-derivative (PID) controller, a peristaltic pump for Ao infusion, a perfusion bioreactor, a pressure head container for LV perfusate retention (2L aspirator bottle with bottom sidearm), and a peristaltic pump to drain excess fluid from the pressure head container and to collect the outflow from PA.

2.2. In the rubber septum, connect the infusion line, pressure-head line, PA-outflow line and bioreactor draining line to the rubber cap surface ports placed on top of the perfusion bioreactor (**Figure 5A**).

2.3. Decellularize hearts under constant pressure of 120 mmHg measured at the aortic root. Mean pressure of the LV should be within 14-18 mmHg throughout the whole decellularization process.

2.4. Decellularize hearts as follows: 4 h of hypertonic solution (500 mM NaCl), 2 h of hypotonic solution (20 mM NaCl), 120 h of sodium dodecyl sulfate (1% SDS) solution, and a final wash with 120 L of 1X PBS (**Figure 6A**).

2.5. Decellularize the hearts under constant pressure control (120 mmHg). Infusion flow rate into Ao is heart-dependent and is, on average, 98.06±16.22 mL/min for hypertonic solution, 76.14±7.90 mL/min for hypotonic solution, 151.50±5.76 mL/min for SDS, and 185.24±7.10 mL/min for PBS. The total consumed volume of each reagent averages 23.36±5.70 L for hypertonic solution and 9.13±1.26 L for hypotonic solution.

2.6. Recirculate the final 60 L of 1% SDS (1 L per gram of heart weight) until the end of SDS perfusion. **Figure 6A** shows a timeline for the decellularization process, eliciting endpoints for data collection: flow rate monitoring (Ao and PA) and outflow collection (PA and non-PA) from pressure head during decellularization.

2.7. Since the SVC and IVC are ligated, it is reasonable to assume that all fluid collected from the PA is the result of actual coronary perfusion (**Figure 5B**). Determine coronary perfusion efficiency by directly dividing the flow rate of perfusate out of the PA by the flow rate of infused solution into Ao:

Coronary perfusion efficiency = $\frac{flow\ rate\ out\ of\ PA}{flow\ rate\ into\ Ao}$ (%).

2.8. Perform comparative analysis of the perfusate obtained from the PA and the LV and the infused solutions in duplicate by loading 200 μL per well in a clear bottom 96-well plate and reading absorbance at 280 nm. The absorbance value, selected empirically after trying different values, was found to give the best normalized values.

2.9. Use the turbidity of clean infused reagent as the control. The turbidity of the outflow perfusate represents washout of cell debris and can be quantified instantly during decellularization as a tracking tool of the process.

2.10. During the final wash with 10 L of 1x PBS, add 500 mL of sterile neutralized 2.1% peracetic acid solution, neutralized with 10N NaOH, leading to a 0.1% peracetic acid solution (v/v) in PBS. Use this solution to sterilize the scaffold.

3. Evaluation of Decellularized Hearts

Note: After decellularization, representative hearts will be used for coronary angiogram imaging and biochemical assays.

3.1. Perform coronary angiography of the representative decellularized human heart to examine the intactness of the coronary vasculature. Briefly, using a fluoroscope, image decellularized human heart after injection of contrast agent through coronary ostial cannula in the main right and left coronary arteries.

3.2. Dissect the decellularized heart to get samples from 19 areas to evaluate the remaining deoxyribonucleic acid (DNA), glycosaminoglycan (GAG) and SDS levels in decellularized tissues. Remove the base of the heart from ventricles and dissect the ventricles into 4 equal sections (**Figure 6C**). Divide each section into the anterior and posterior right ventricle (RV), the anterior and posterior LV, and the interventricular septum (IVS). The tissue containing the apex is dissected into the LV and RV for sampling.

3.3. Cut tissue samples for DNA, GAG and SDS assays (~15 mg of wet weight).

3.4. Extract double-stranded DNA (dsDNA) by digesting samples in 1 M NaOH for 3 h at 65 °C and adjust pH to 7 using 10x Tris-EDTA (TE) buffer and 1 M hydrochloric acid (HCl).

3.5. Quantify dsDNA using a dsDNA Assay kit with a calf thymus standard (see **Table of Materials**). Read samples in duplicate using a fluorescence microplate reader (excitation at 480 nm and emission at 520 nm). Calculate the percentage of residual dsDNA in the decellularized hearts by comparing dsDNA concentration in each tissue to that in cadaveric (% cadaveric).

3.6. Obtain sulfated GAGs into solution by digesting tissue samples in a papain extraction solution (0.2 M sodium phosphate buffer with EDTA disodium salt, cysteine HCl, sodium acetate, and papain) at 65 °C for 3 hours. Measure GAG content (in duplicate) by using a Glycosaminoglycan Assay Kit.

3.7. Lyophilize samples for SDS assay in a heated vacuum and measure dry weight. Add 200 µL of ultrapure water to each dried sample and homogenize to extract the residual SDS into solution. Mix this SDS solution to chloroform and a methylene blue solution (12 mg of methylene blue in 1 L of 0.01 M HCl). The SDS will separate in the organic layer by binding to the methylene blue dye.

3.8. Using a fluorescence microplate reader, read the absorbance (655 nm) of the standards and samples in duplicate to calculate the residual SDS. Normalize this SDS value to tissue dry weight.

3.9. Image samples from thick regions (*i.e.,* LV, RV and septum) of human heart with nonlinear optical microscopy (NLOM) to confirm cellular removal after decellularization. The NLOM setup is detailed in our previous publications[18-20]. NLOM enables us to image cell, elastin, collagen and myosin fibers through its two-photon fluorescence (TPF) and second harmonic generation (SHG) channels without using any exogenous stain or dye[21].

REPRESENTATIVE RESULTS:

After a 7-day decellularization with antegrade aortic perfusion under constant pressure of 120 mmHg, the human heart turned translucent (**Figure 6B**). The heart was grossly dissected into 19 sections for biochemical (DNA, GAG and SDS) analysis (**Figure 6C**) to evaluate the final decellularized product.

Throughout the decellularization process, infusion flow rate of different solutions varied as the pressure was kept constant. The flow rate into the Ao (**Figure 7A**) gradually decreased from 96.68±23.54 to 80.59±12.41 mL/min (16.64%) as the perfusion solution changed from hypertonic to hypotonic. In contrast, flow rate increased from 71.68±10.63 to 110.61±14.40 mL/min (54.31%) when perfusion solution changed from hypotonic to SDS. During the SDS perfusion, infusion flow rate fluctuated between 110±14.40 and 176.31±44.03 mL/min. The outflow rate from PA (**Figure 7B**) initially showed a similar trend (**Figure 7A**). However, the outflow rate during 1% SDS perfusion decreased from 35.77±9.07 to 27.08±4.09 mL/min. Coronary perfusion efficiency was used to evaluate aortic valve patency and similar trends. Efficiency decreased over

time as different reagents perfused through the vasculature (**Figure 7C**). During the first hour of the 1X PBS wash, perfusion efficiency was restored to the original pre-hypotonic solution value (28.39±3.61% at 1-h PBS *vs.* 31.02±7.16% at 1-h hypotonic). The mean coronary perfusion efficiencies were 46.08±9.89%, 28.08±7.12%, 25.70±5.30%, and 28.39±3.61% with the hypertonic solution, the hypotonic solution, 1% SDS, and 1X PBS, respectively (**Figure 7D**).

Since the outflow perfusate from PA and LV were simultaneously collected, their debris content could be compared (**Figure 8A**) by spectroscopy absorbance measured at 280 nm (**Figure 8B**). The turbidity of the effluent from PA and LV decreased over time during perfusion of each solution; however, turbidity from the PA showed a more abrupt color change as compared to that observed from LV during the initial perfusion period. After switching from a hypertonic to a hypotonic solution, the turbidity of PA outflow changed from 1.15±0.03 to 1.40±0.07 (21.73% increase) and of LV changed from 1.13±0.05 to 1.24±0.07 (9.73% increase). During the first hour of 1% SDS perfusion, turbidity changed from 1.17±0.04 to 2.77±0.15 (136.75% increase) for PA and 1.11±0.04 to 1.75±0.26 (56.65% increase) for the LV effluent. The correlation between outflow turbidity and cell debris washout was evaluated using the bicinchoninic acid (BCA) protein assay when protein concentration was quantified in the outflow samples. The results obtained from the decellularization of 6 human hearts revealed a linear correlation between protein concentration and effluent turbidity with $R^2 = 0.95$ (**Figure 8C**).

After completion of whole-heart decellularization, the coronary angiogram confirmed the preservation of intact coronary vasculature (**Figure 9**). Nonlinear optical imaging of myocardium layers from thick areas (*i.e.,* RV, LV, and septum) in decellularized human heart confirmed cell removal, as no cell presence was observed in TPF channels (**Figure 10**). Cells (*i.e.,* cardiomyocytes or cardiac fibroblasts) with their autofluorescence can be easily identified in TPF channel by their oval and elongated shape morphologies. To ensure effectiveness of the decellularization process and cellular debris removal, the decellularized human hearts were further grossed into 19 regions (**Figure 6C**) to quantify the levels of DNA, sulfated GAGs, and SDS remaining in those regions. DNA in all regions was less than 10% of cadaveric heart. DNA in right atrium (8.39%-10.38% relative to cadaveric) and left atrium (5.11%-7.60%) was highest (**Figure 11A**).

FIGURE LEGENDS:

Figure 1: Cadaveric human heart from an organ procurement agency. Anterior and posterior views of cadaveric human heart. Inferior vena cava and a portion of right atrium are missing, as observed in dashed region.

Figure 2: Inspection for septal and/or valve anatomical anomalies. (A) Inspect if patent foramen ovale (PFO) is present (communication between right and left atrium). **(B)** A 5-0 polypropylene suture is applied in a continuous fashion to close PFO. **(C)** Right atrium is closed with a running suture of 5-0 polypropylene. **(D)** The main pulmonary artery is dissected away from the ascending aorta by blunt dissection. FO: foramen ovale; PA: pulmonary artery; Ao: aorta.

Figure 3: Components of the infusion bioreactor. The decellularization system is composed of **(A)** rubber cap with 4 ports; **(B)** outflow line to be connected to the pulmonary artery (PA); **(C, F)** connectors with luer lock for PA and aorta (Ao), **(D)** insertion line for the left ventricle (LV), **(E)** infusion line to be connected to the aorta, **(G)** polyester pouch, and **(H)** Perfusion container.

Figure 4: Human heart cannulation and infusion bioreactor assembly. (A) Anterior view of the heart showing pulmonary artery (PA) and aorta (Ao) individually cannulated. **(B)** Posterior view of the heart showing cannula directed to left ventricle (LV) through pulmonary vein (PV). **(C)** Human heart inside the Infusion bioreactor after assembly.

Figure 5: System setup of inverted oriented decellularization with pressure head. (A) The complete decellularization system is composed of: a computer, a proportional-integral-derivative (PID) controller, pumps, a bioreactor, and reservoirs for collecting the effluent from pulmonary artery (PA) and left ventricle (LV). Ao: aorta. Arrows indicate flow direction. **(B)** The schematic of the setup of human heart inside perfusion bioreactor and the associated flow paths of perfusate/effluent during decellularization.

Figure 6: Schematic representation of the decellularization procedure and post-decellularization examination of a human heart. (A) Diagram of the decellularization procedure. **(B)** Anterior and posterior examination of a decellularized human heart. **(C)** Gross dissection of a human heart into four cross-sections (section A to section D) for biochemical assay analysis. The coloring in the human hearts is caused by residual lipofucin deposition. The coloring normally presents in inner ventricular surface or the boundary between epicardium and myocardium. LA: left atrium; RA: right atrium; LV: left ventricle; RV: right ventricle; Ant: anterior; Post: posterior; Hyper: hypertonic; Hypo: hypotonic; SDS: sodium dodecyl sulfate; PBS: phosphate buffered saline.

Figure 7: Time-lapse flow dynamics during decellularization. (A) Infusion flow rate of decellularization solutions into aorta during procedure. **(B)** Flow rate of effluent from PA during decellularization. **(C)** Coronary perfusion efficiency during decellularization. **(D)** Mean coronary perfusion efficiency during perfusion of different solutions/reagents. N = 6. Data represent mean±SEM. PA: pulmonary artery; Hyper: hypertonic; Hypo: hypotonic; SDS: sodium dodecyl sulfate; PBS: phosphate buffered saline; SEM: standard error of mean.

Figure 8: Time-lapse cell debris washout during decellularization. (A) Outflow media collection from PA and non-PA (Left ventricle). **(B)** Result of turbidity measurement at 280 nm. **(C)** Linear correlation exists between protein concentration and turbidity. n = 6 human hearts. Control was clean decellularization solution. Data represent mean±SEM. PA: pulmonary artery; Hyper: hypertonic; Hypo: hypotonic; SDS: sodium dodecyl sulfate; SEM: standard error of mean.

Figure 9: Coronary angiogram of decellularized human heart confirms the vascular patency after decellularization.

Figure 10: Images obtained using nonlinear optical microscopy from cadaveric and decellularized myocardium show no presense of cells (*i.e.,* cardiomyocytes or cardiac fibroblasts) with oval or elongated shape morphologies in the decellularized LV, RV and septum. LV: left ventricle; RV: right ventricle; TPF: two photon fluorescence; SHG: second harmonic generation. Some cardiac cells are indicated by arrows.

Figure 11: Biochemical assay results. (A) Remaining DNA relative to cadaveric heart in decellularized tissues. **(B)** Remaining GAG relative to cadaveric heart in decellularized tissues. **(C)** Remaining SDS in decellularized tissues. n = 6 human hearts. Data represent mean±SEM. LA: left atrium; RA: right atrium; LV: left ventricle; RV: right ventricle; Ant: anterior; Post: posterior; SDS: sodium dodecyl sulfate; SEM: standard error of mean.

Table 1: A summary of pros and cons of whole-heart decellularization using conventional upright perfusion vs. inverted Langendorff perfusion inside a pressurized pouch.

DISCUSSION:

To our knowledge, this is the first study to report inverted decellularization of human hearts inside a pressurized pouch with time-lapse monitoring of flow rate and cell debris removal. The pericardium-like pouch keeps the orientation of the heart stable throughout the decellularization procedure. Submerging and inverting the whole hearts inside a pouch prevents dehydration and minimizes excessive strain on the aorta (from heart weight) when compared to the conventional upright Langendorff perfusion decellularization method[9]. This, in turn, preserves the competency of the aortic valve.

To achieve maximal decellularization efficiency, coronary vascular resistance must be low to ensure adequate and consistent perfusion of fluid through the entire myocardium. In the whole-heart decellularization model using retrograde perfusion, fluid accumulates in the ventricles and elevates intraventricular pressure, which, in turn, increases coronary vascular resistance and limits the flow of fluids. Even though the aortic valve is intact, the ventricular cavity fills secondary to physiological leakage and in turn compresses the ventricular wall.

Our technique of decellularizing a heart inside a pressurized pouch is aimed to alleviate this problem and increase decellularization efficiency. A pressure of 120 mmHg at the aortic root and 14 mmHg in the pouch is maintained throughout the decellularization process. These pressure values are very close to physiological range (80-120 mmHg in aorta and 15 mmHg for Left ventricular end-diastolic pressure[22]). According to Murthy *et al.*[23], the myocardial blood flow rate ranges from 0.61 to 1.10 mL/min/g, and the human heart weight[24,25] is about 245 to 308 g; hence, the physiological coronary flow rate is about 149.45 to 338.80 mL/min, but depends on heart weight. Our outflow rate from PA ranged from 20 to 50 mL/min, which is less than the value of physiological coronary flow rate and could have resulted from 2 different situations: 1) the infusion of solutions to the heart produce edema and there is also normal anatomical drainage of the coronary system to the left ventricle cavity; 2) as the decellularization occurs, liquid is also lost through the decellularized walls due to a natural increase in their permeability. This pressure differential prevents collapse of the vessels and allows them to remain patent. Moreover, this

system maintains the heart in relative anatomic conditions without compressing the myocardial wall, which would increase coronary vascular resistance and impair the intravascular circulation of the decellularization solutions. The infusion flow rate profile of human hearts (**Figure 7A**) is very similar to what we observed in our inverted decellularization of porcine heart[9], with lowest infusion flow rate occurring during the hypotonic perfusion and a slight increase in flow rate (110.61±14.40 mL/min to 176.31±44.03 mL/min) occurring during 1% SDS perfusion. Our infusion flow rate (mean value=151.50±3.71 mL/min) during 1% SDS perfusion was comparable to, or even less than that for human heart decellularization reported by Guyette *et al.*[14] However, our method is performed with pressure control of 120 mmHg and their method used 60 mmHg. This difference in perfusion pressures suggests a superior effectiveness of aortic valve closure in our technique since a lower infusion flow rate could maintain higher pressure. Another possibility is that the increased coronary resistance was due to the applied 14 mmHg pressure inside the pouch. Additionally, our human heart method showed a similar trend of decreasing coronary perfusion efficiency (~30%, **Figure 7C**, **7D**) from hyper to hypotonic solution change when compared to our inverted porcine heart decellularization (~10% in inverted orientation[9] *vs.* 1-2% in upright orientation). However, this novel method could preserve coronary perfusion efficiency during SDS perfusion comparable to solution perfusion and thus appears superior to our prior method of sample inversion. **Table 1** lists the pros and cons of conventional upright perfusion *vs.* inverted Langendorff perfusion inside a pressurized pouch.

In addition to flow rate, outflow turbidity monitoring could be another useful tool to evaluate decellularization progress and efficiency. During decellularization, turbidity of the effluent from the PA was higher than that of the effluent from non-PA sites (**Figure 8B**). This suggests that most of the perfused solution was going through the vasculature for "proper" decellularization. Yet for this to be valid, the following must be addressed: inter-chamber shunts, or patency of the aortic valve. Careful and meticulous inspection is therefore needed to prevent failure of the method due to anatomical non-conformities. The turbidity profile (**Figure 8B**) of the whole heart decellularization process demonstrated similar trends as previously shown, with abrupt turbidity change during the initial transition period of different perfusates[9].

A main goal for decellularized tissues is to be able to repopulate them with cells and achieve high cell attachment, proliferation, maturation and functionality. Our decellularized tissues have been successfully cellularized for various applications[26,27], where the tissues were successfully cellularized and achieved lower thrombogenicity. In our biochemical analyses of decellularized human hearts, we evaluated 19 regions with different tissue thicknesses. The DNA and SDS in decellularized tissues varied, with the highest value obtained in the right and left atrium. This could be caused by the orientation of the heart in an upside-down configuration, wherein cell debris was trapped at the bottom of the pouch or where external pressure reduced flow. Perfusion decellularization relies on undamaged heart structures, including intact coronaries and tributaries. As these organs are procured from multi-organ donors, these hearts usually have a large portion of their atria removed. During the preparation of these organs and repair of the atrial wall, there was disruption in the irrigation of these regions, jeopardizing the flow of the decellularization solutions. For non-perfusion heart decellularization, other research groups have reported 2-6% leftover DNA in rat[28], porcine[29,30] and human[31] as compared with respective

cadaveric heart. However, they used freeze-thaw[28-30], enzyme[29,30] and serum[31] in their decellularization protocol, which may damage the ECM to a greater degree than our perfusion-based technique. Developing methods to adequately address these limitations will be critical.

ACKNOWLEDGMENTS:

This research was supported by the Houston Endowment grant and the Texas Emerging Technology Fund. The authors acknowledge the organ procurement agency LifeGift, Inc. and the donor's families for making this study possible.

DISCLOSURES:

Dr. Taylor is the founder and shareholder in Miromatrix Medical, Inc. This relationship is managed in accordance with the conflict of interest policies by the University of Minnesota and Texas Heart Institute; the other authors have no conflict of interest to disclose.

REFERENCES:

1 Writing Group Members, *et al.* Executive Summary: Heart Disease and Stroke Statistics--2016 Update: A Report From the American Heart Association. *Circulation.* **133** (4), 447-454, (2016).

2 Zia, S. *et al.* Hearts beating through decellularized scaffolds: whole-organ engineering for cardiac regeneration and transplantation. *Critical Reviews in Biotechnology.* **36** (4), 705-715, (2016).

3 Zimmermann, W. H. Strip and Dress the Human Heart. *Circulation Research.* **118** (1), 12-13, (2016).

4 Ott, H. C. *et al.* Perfusion-decellularized matrix: Using nature's platform to engineer a bioartificial heart. *Nature Medicine.* **14** (2), 213-221, (2008).

5 Sanchez, P. L. *et al.* Acellular human heart matrix: A critical step toward whole heart grafts. *Biomaterials.* **61** 279-289, (2015).

6 Peloso, A. *et al.* Current achievements and future perspectives in whole-organ bioengineering. *Stem Cell Research & Therapy.* **6** 107, (2015).

7 Guyette, J. P. *et al.* Perfusion decellularization of whole organs. *Nature Protocols.* **9** (6), 1451-1468, (2014).

8 Momtahan, N., Sukavaneshvar, S., Roeder, B. L. & Cook, A. D. Strategies and Processes to Decellularize and Cellularize Hearts to Generate Functional Organs and Reduce the Risk of Thrombosis. *Tissue Engineering Part B-Reviews.* **21** (1), 115-132, (2015).

9 Lee, P. F. *et al.* Inverted orientation improves decellularization of whole porcine hearts. *Acta Biomaterialia.* 10.1016/j.actbio.2016.11.047, (2016).

10 Momtahan, N. *et al.* Automation of Pressure Control Improves Whole Porcine Heart Decellularization. *Tissue Eng Part C Methods.* 10.1089/ten.TEC.2014.0709, (2015).

11 Weymann, A. *et al.* Development and Evaluation of a Perfusion Decellularization Porcine Heart Model - Generation of 3-Dimensional Myocardial Neoscaffolds. *Circulation Journal.* **75** (4), 852-860, (2011).

12 Weymann, A. *et al.* Bioartificial heart: A human-sized porcine model--the way ahead. *PLoS One.* **9** (11), e111591, (2014).

13 Remlinger, N. T., Wearden, P. D. & Gilbert, T. W. Procedure for decellularization of porcine heart by retrograde coronary perfusion. *Journal of Visualized Experiments.* 10.3791/50059 (70), e50059, (2012).
14 Guyette, J. P. *et al.* Bioengineering Human Myocardium on Native Extracellular Matrix. *Circulation Research.* **118** (1), 56-72, (2016).
15 Sanchez, P. L. *et al.* Data from acellular human heart matrix. *Data Brief.* **8** 211-219, (2016).
16 Garreta, E. *et al.* Myocardial commitment from human pluripotent stem cells: Rapid production of human heart grafts. *Biomaterials.* **98** 64-78, (2016).
17 Wainwright, J. M. *et al.* Preparation of Cardiac Extracellular Matrix from an Intact Porcine Heart. *Tissue Engineering Part C-Methods.* **16** (3), 525-532, (2010).
18 Larson, A. M. & Yeh, A. T. *Ex vivo* characterization of sub-10-fs pulses. *Optics Letters.* **31** (11), 1681-1683, (2006).
19 Lee, P. F., Yeh, A. T. & Bayless, K. J. Nonlinear optical microscopy reveals invading endothelial cells anisotropically alter three-dimensional collagen matrices. *Experimental Cell Research.* **315** (3), 396-410, (2009).
20 Lee, P. F., Bai, Y., Smith, R. L., Bayless, K. J. & Yeh, A. T. Angiogenic responses are enhanced in mechanically and microscopically characterized, microbial transglutaminase crosslinked collagen matrices with increased stiffness. *Acta Biomaterialia.* **9** (7), 7178-7190, (2013).
21 Wu, Z. *et al.* Multi-photon microscopy in cardiovascular research. *Methods.* **130** 79-89, (2017).
22 Ramanathan, T. S., H. Coronary blood flow. *Continuing Education in Anaesthesia Critical Care & Pain.* **5** (2), 61-64, (2005).
23 Murthy, V. L. *et al.* Clinical Quantification of Myocardial Blood Flow Using PET: Joint Position Paper of the SNMMI Cardiovascular Council and the ASNC. *Journal of Nuclear Cardiology.* **25** (1), 269-297, (2018).
24 Molina, D. K. & DiMaio, V. J. Normal organ weights in men: Part I-the heart. *The American Journal of Forensic Medicine and Pathology.* **33** (4), 362-367, (2012).
25 Molina, D. K. & DiMaio, V. J. Normal Organ Weights in Women: Part I-The Heart. *The American Journal of Forensic Medicine and Pathology.* **36** (3), 176-181, (2015).
26 Robertson, M. J., Dries-Devlin, J. L., Kren, S. M., Burchfield, J. S. & Taylor, D. A. Optimizing cellularization of whole decellularized heart extracellular matrix. *PLoS One.* **9** (2), e90406, (2014).
27 Robertson, M. J., Soibam, B., O'Leary, J. G., Sampaio, L. C. & Taylor, D. A. Cellularization of rat liver: An *in vitro* model for assessing human drug metabolism and liver biology. *PLoS One.* **13** (1), e0191892, (2018).
28 Baghalishahi, M. *et al.* Cardiac extracellular matrix hydrogel together with or without inducer cocktail improves human adipose tissue-derived stem cells differentiation into cardiomyocyte-like cells. *Biochemical and Biophysical Research Communications.* 10.1016/j.bbrc.2018.05.147, (2018).
29 Perea-Gil, I. *et al. In vitro* comparative study of two decellularization protocols in search of an optimal myocardial scaffold for cellularization. *American Journal of Translational Research.* **7** (3), 558-573, (2015).

30 Freytes, D. O., O'Neill, J. D., Duan-Arnold, Y., Wrona, E. A. & Vunjak-Novakovic, G. Natural cardiac extracellular matrix hydrogels for cultivation of human stem cell-derived cardiomyocytes. *Methods Molecular Biology.* **1181** 69-81, (2014).

31 Oberwallner, B. *et al.* Preparation of cardiac extracellular matrix scaffolds by decellularization of human myocardium. *Journal of Biomedical Materials Research Part A.* **102** (9), 3263-3272, (2014).

Figure

Click here to download Figure Fig 1.tif

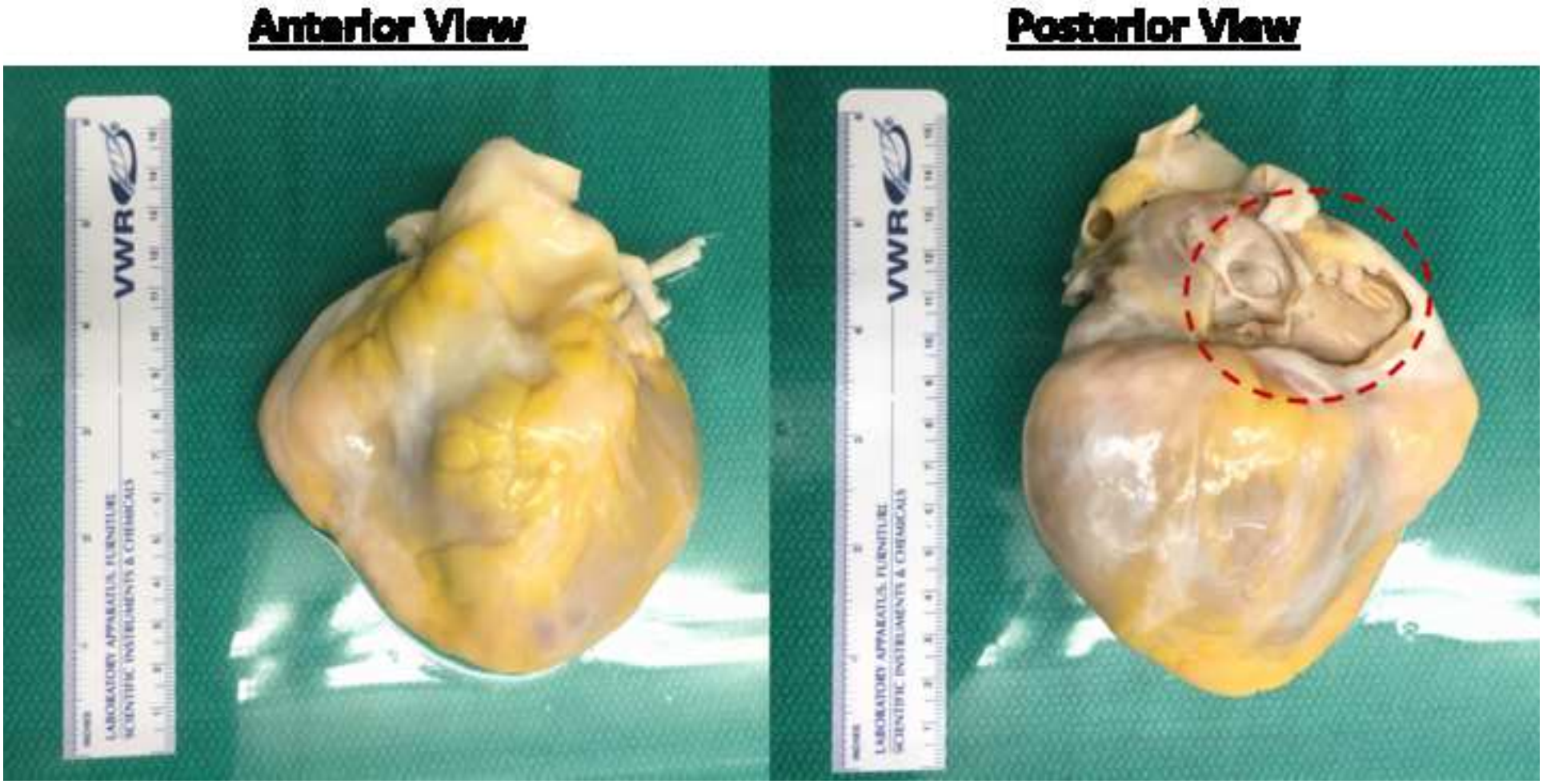

Figure

Click here to download Figure Fig 2.tif

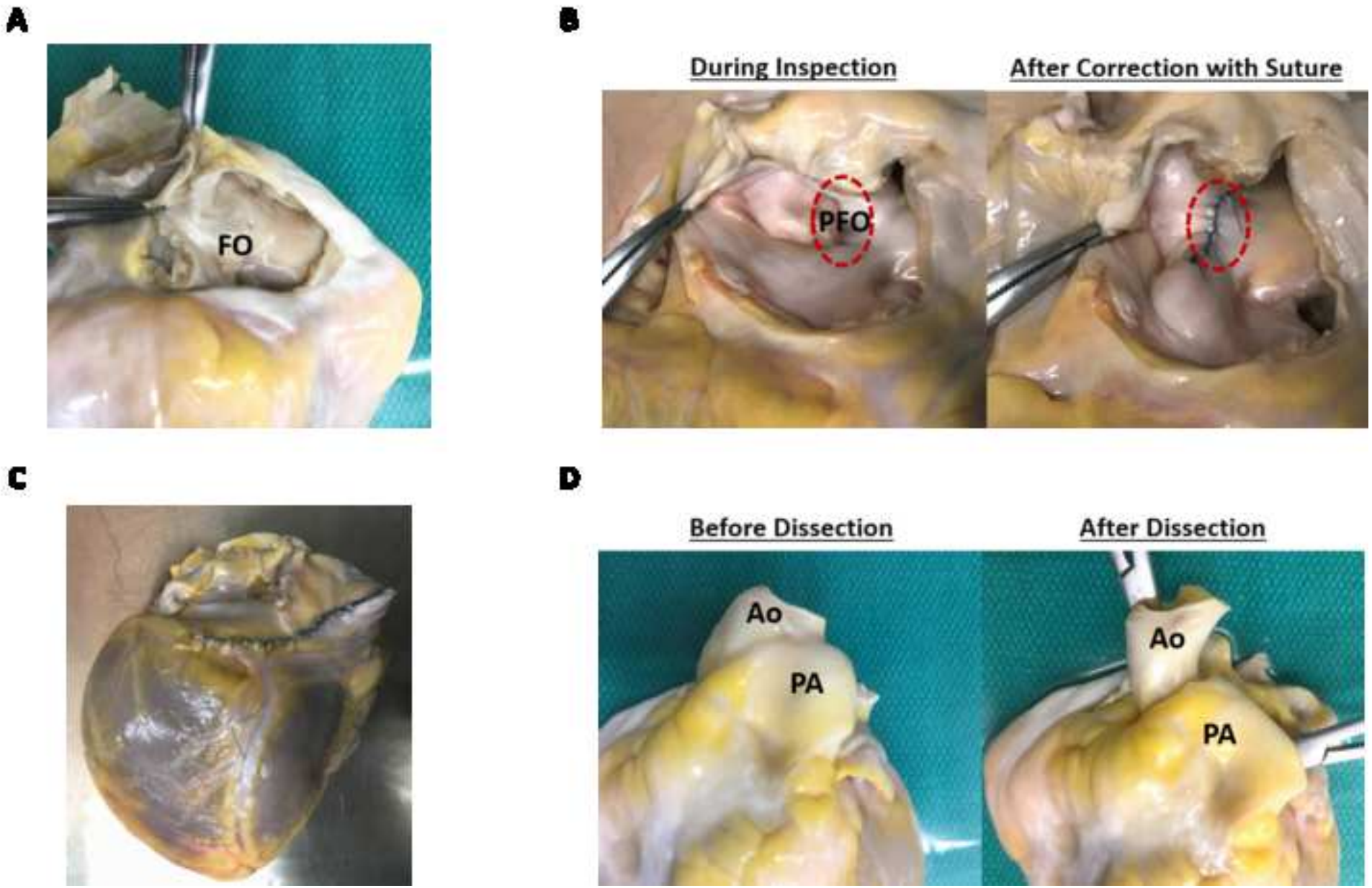

Figure

Click here to download Figure Fig 3.tif

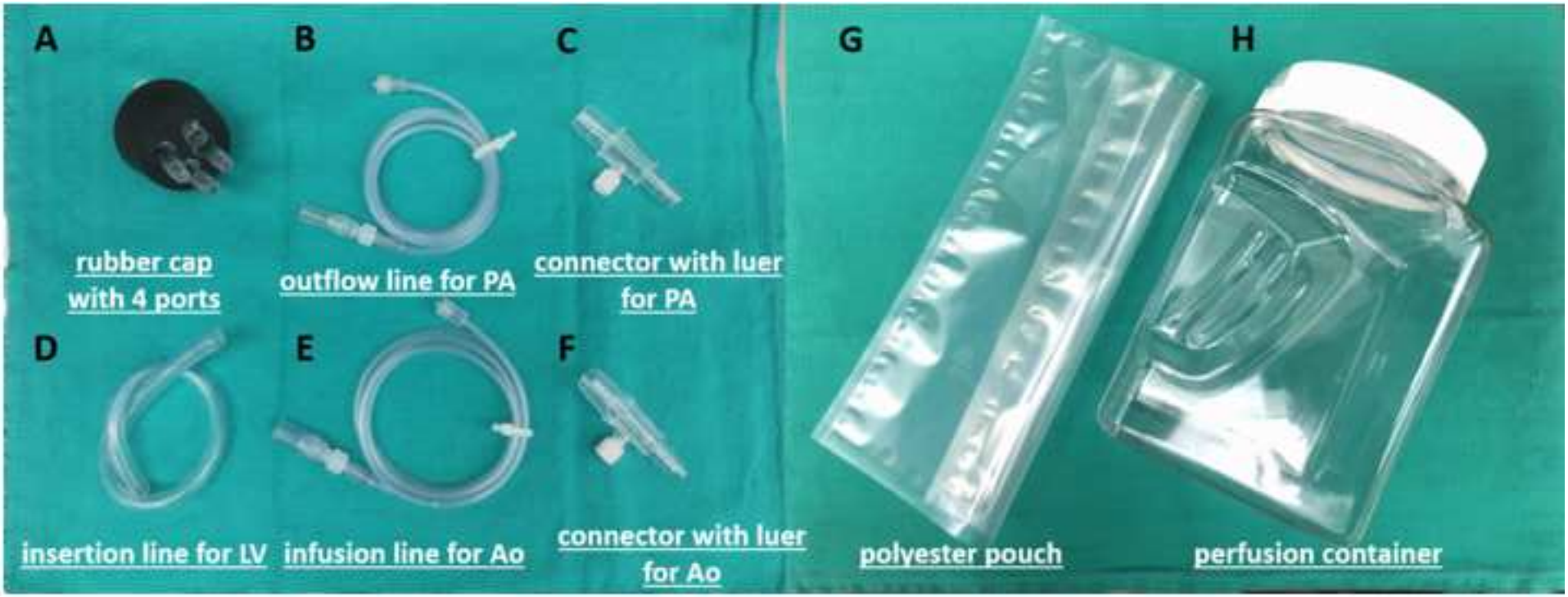

Figure 4

Click here to download Figure Fig 4.tif

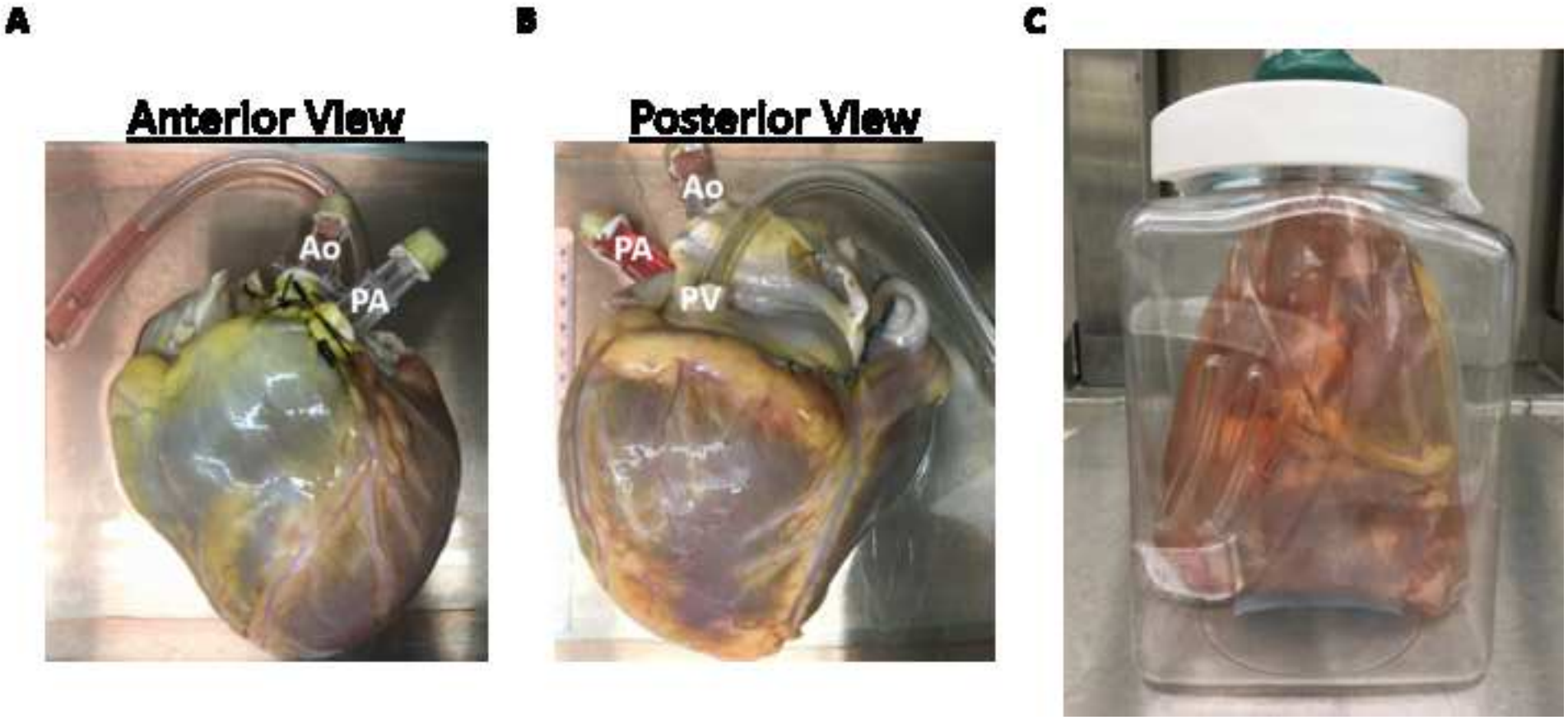

Figure 5

Click here to download Figure Fig 5.tif

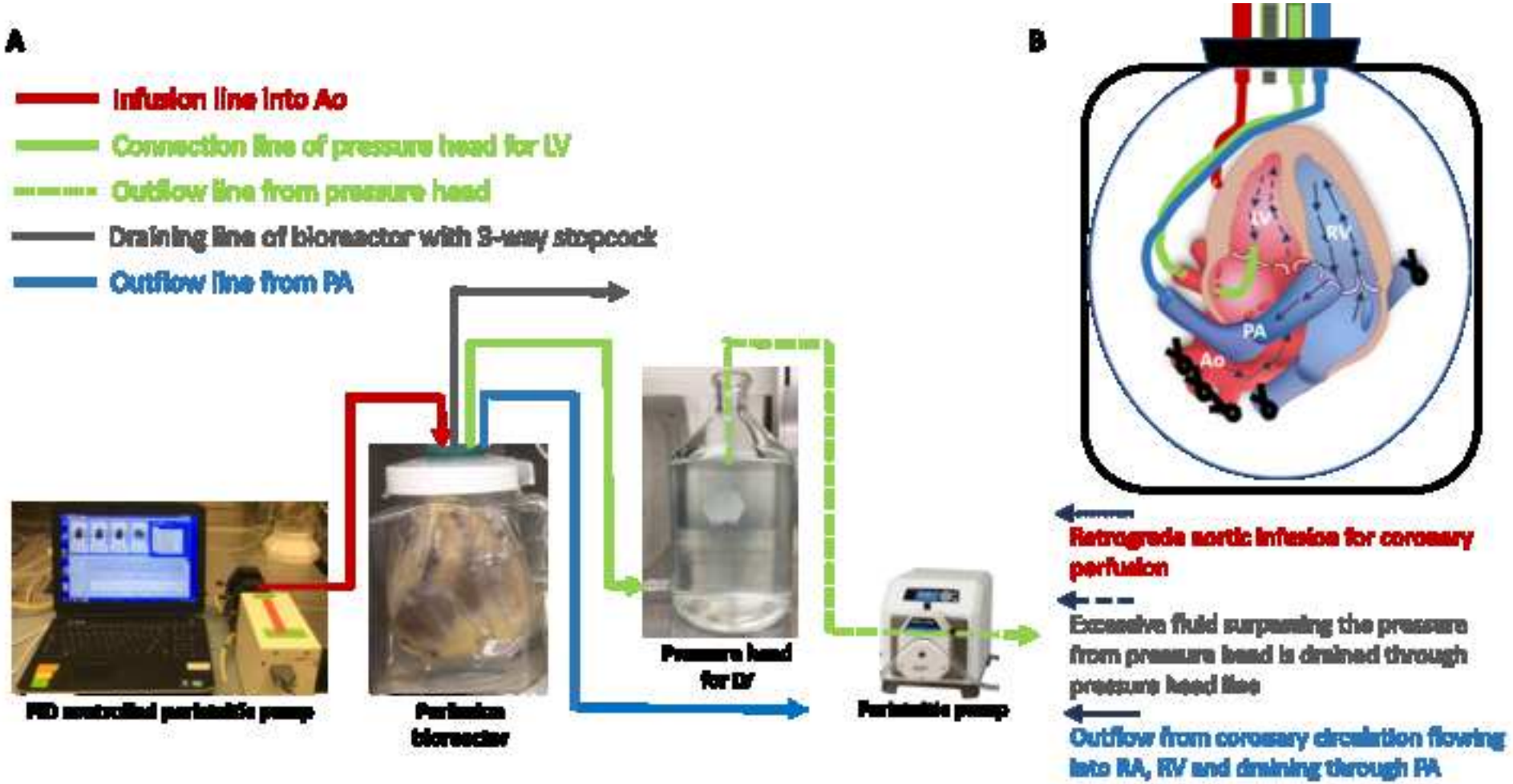

Figure 6

Click here to download Figure Fig 6.tif

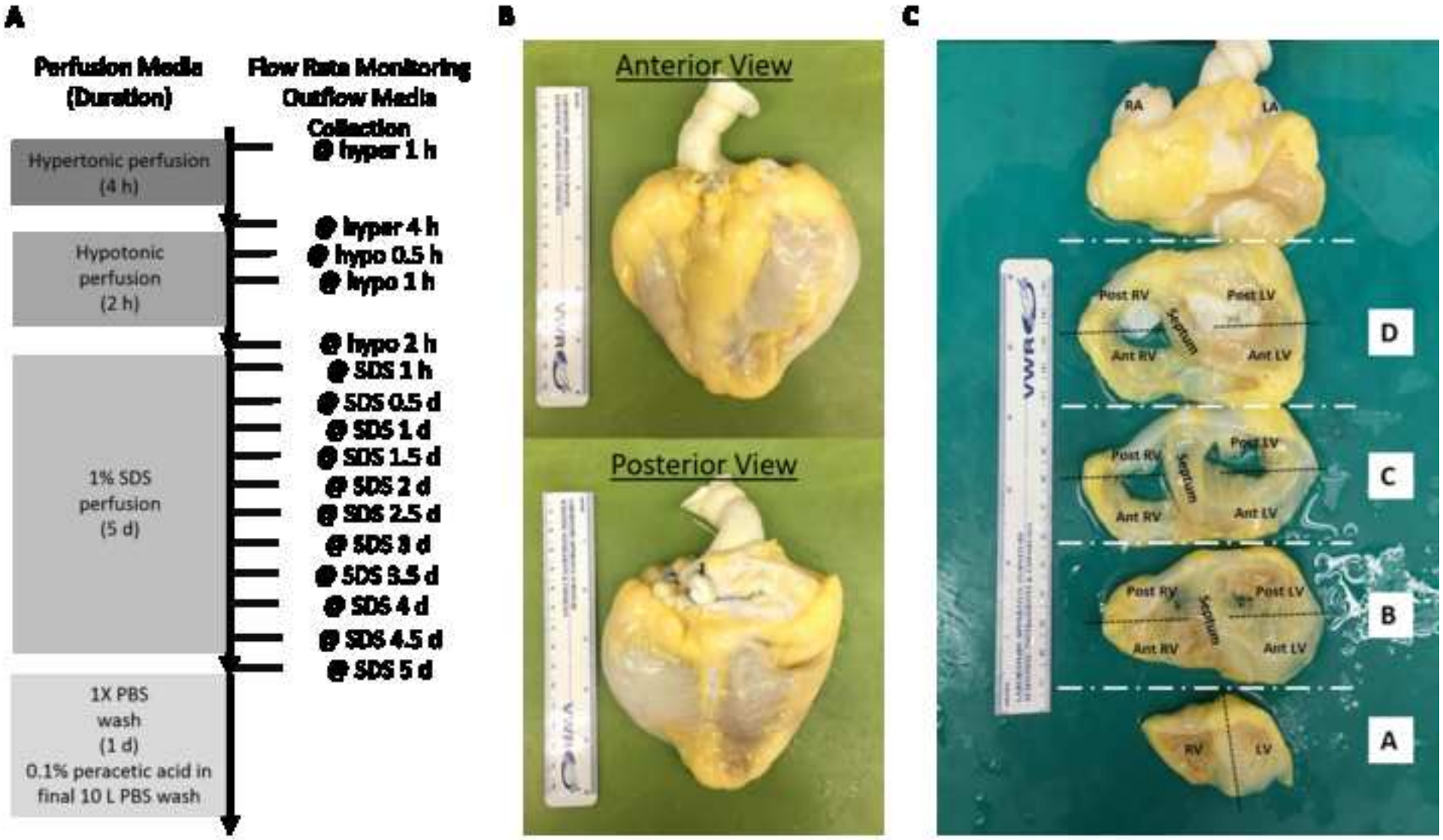

Figure

Click here to download Figure Fig 7 high res.tif

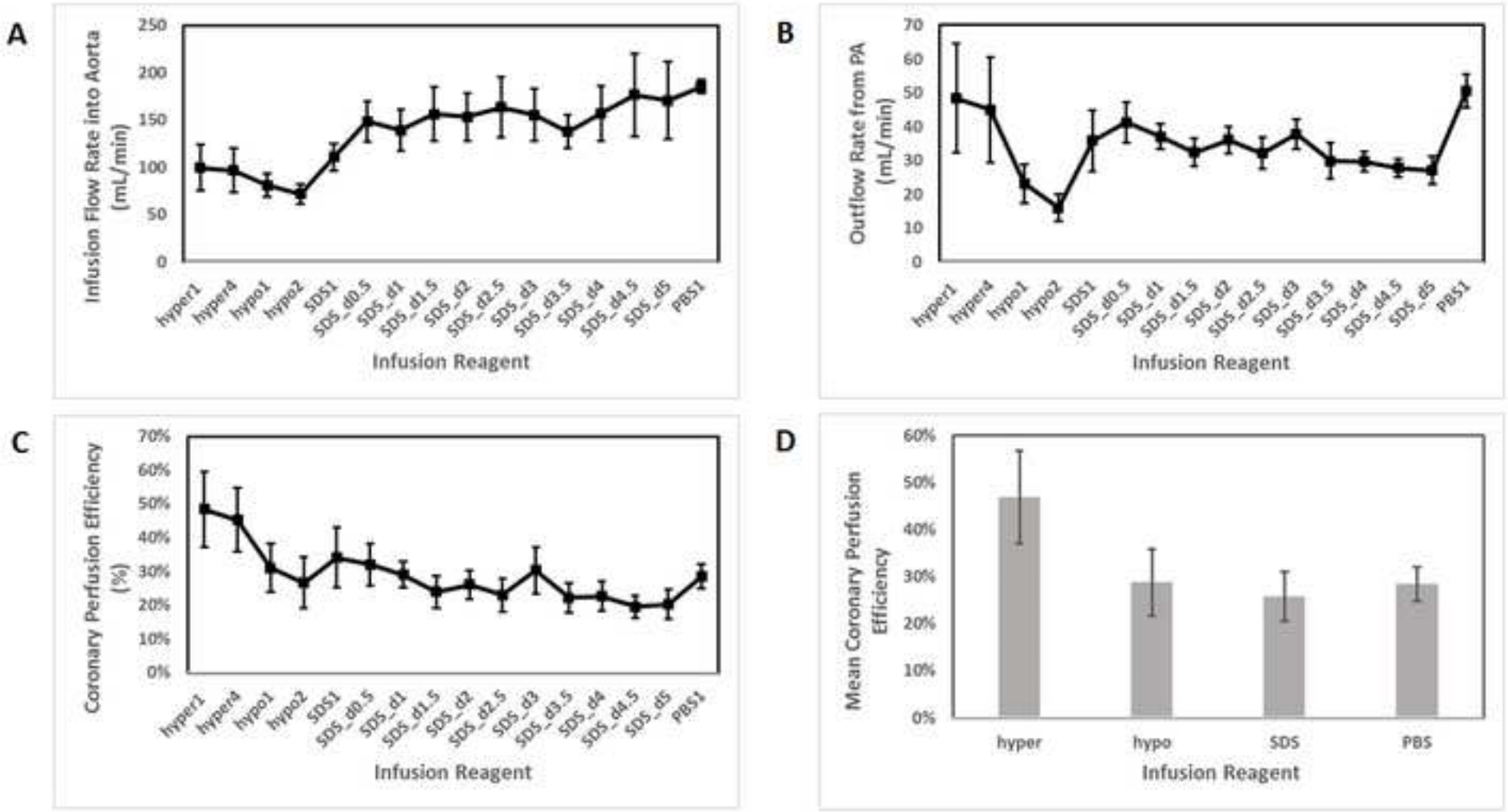

Figure

Click here to download Figure Fig 8 high res.tif

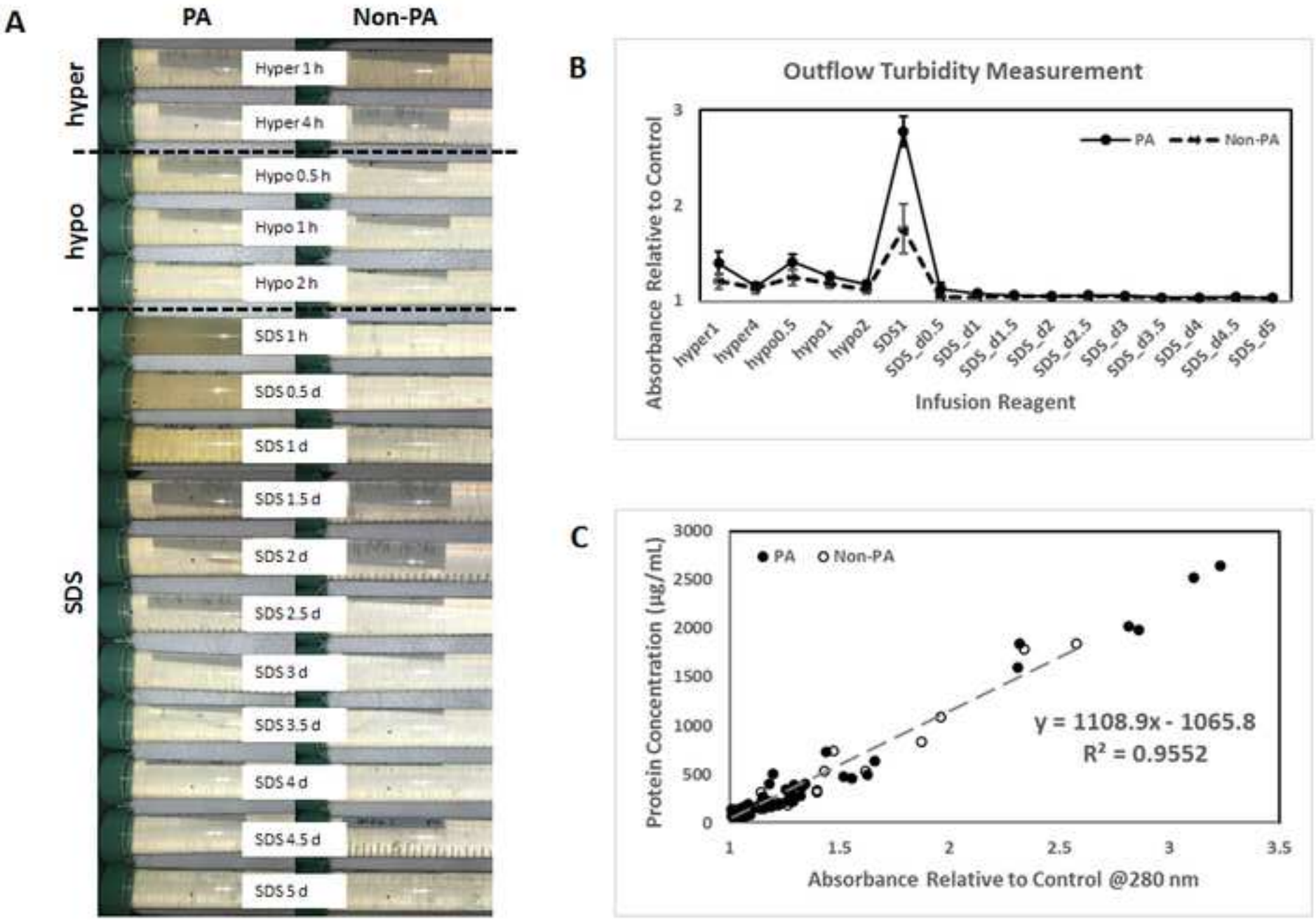

Figure

Click here to download Figure Fig 9.tif

Figure 10

Click here to download Figure Fig 10.tif

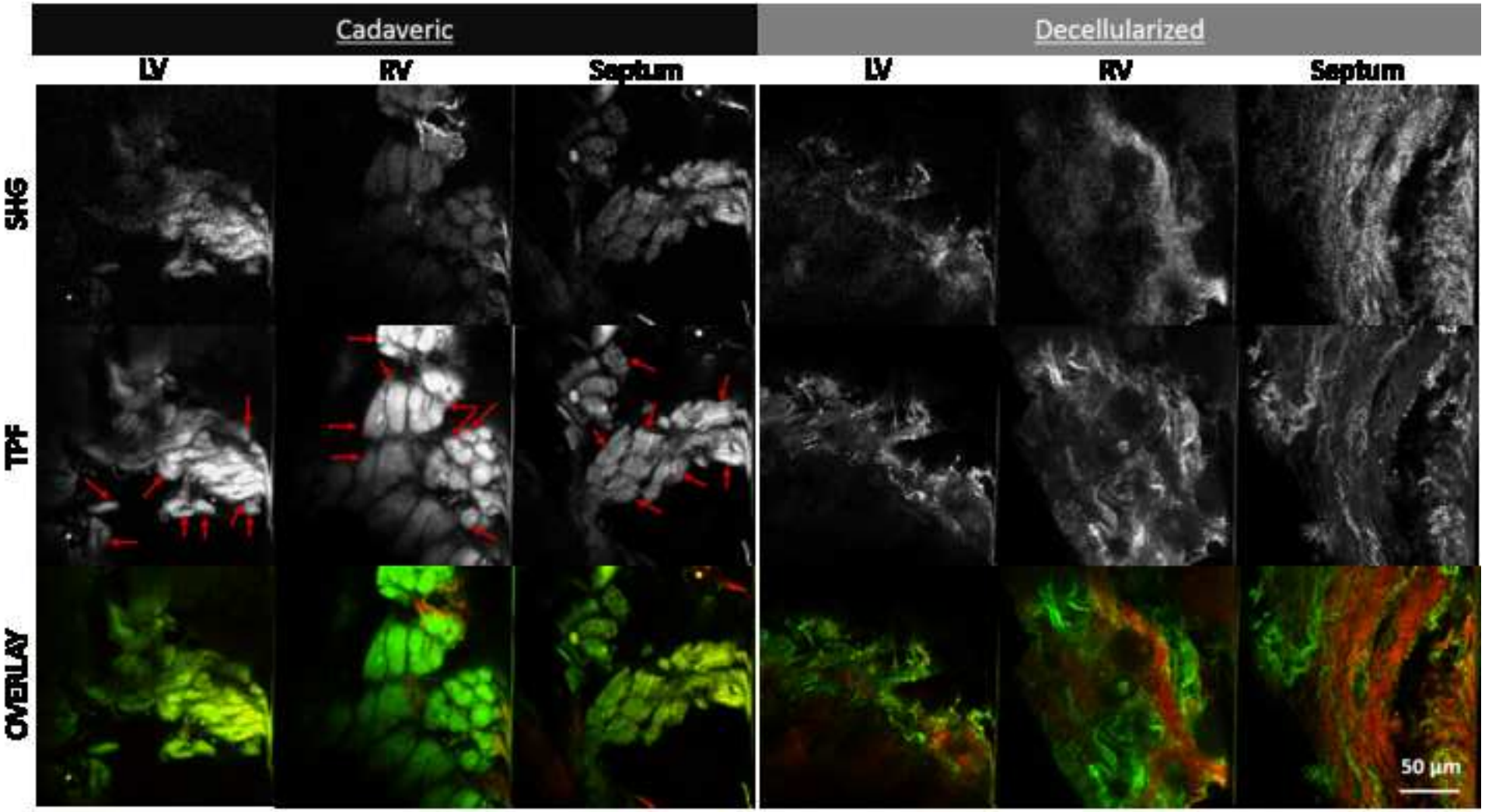

Figure

Click here to download Figure Fig 11 high res.tif

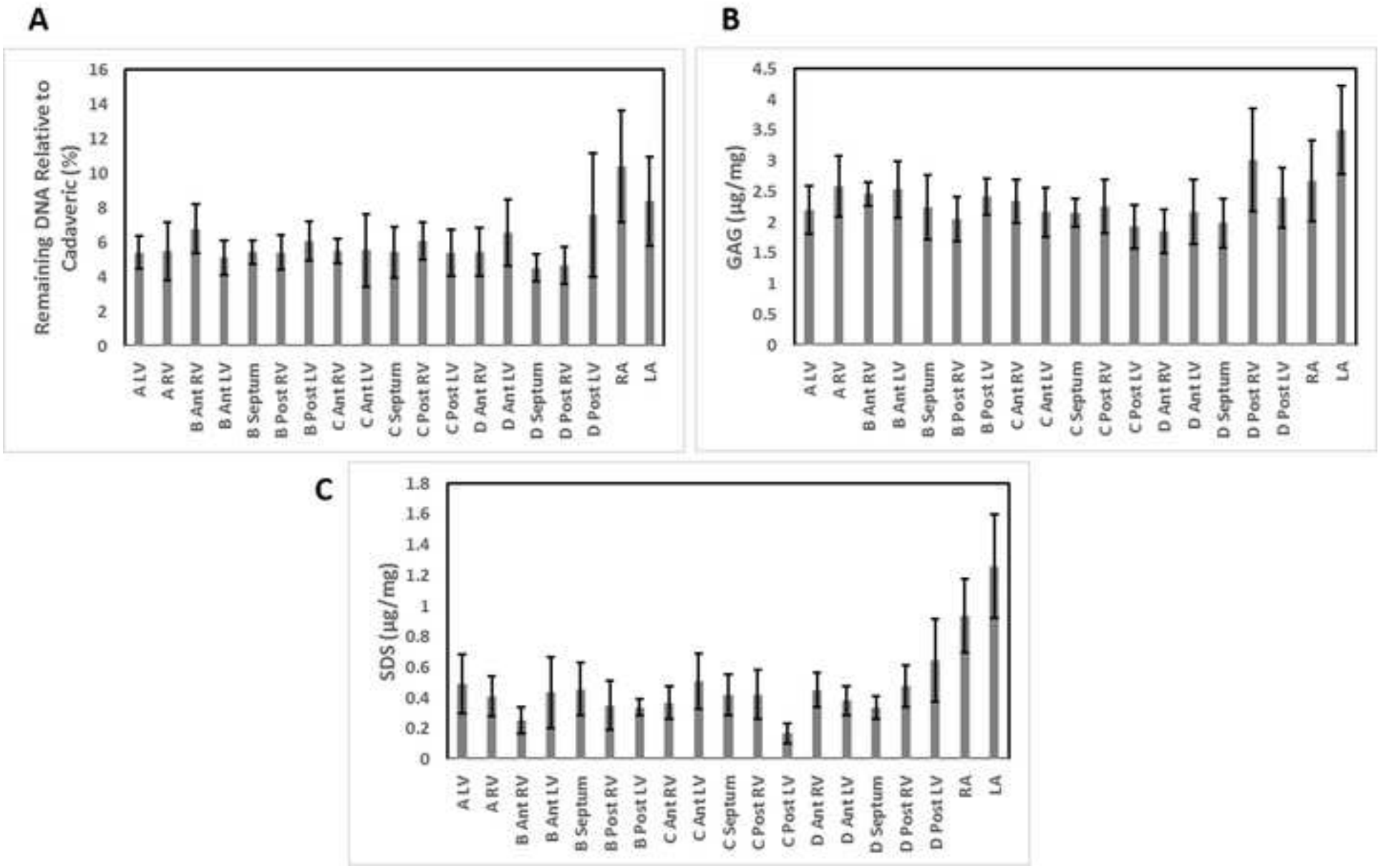

Table 1

Method
Conventional upright Langendorff perfusion
Inverted Langendorff perfusion inside a pressurized pouch

Pro
• Easy to access the heart to repair during decellularization
• Minimize strain exerted on the aorta owing to heart weight • Low infusion flow rate during SDS perfusion under constant pressure control • Improved coronary perfusion efficiency during SDS perfusion • No tissues will be dried out since the whole heart is submerged/hydrated.

Con
• Excessive strain on the aorta owing to heart weight • High infusion flow rate during SDS perfusion under constant pressure control • Low coronary perfusion efficiency during SDS perfusion • The portion of aorta/pulmonary artery above cannula ligation line could get dehydrated and easily contaminated
• Hard to access the heart if repairing is needed.

Table of Materials

Click here to download Table of Materials JoVE materials list v2 062618.xlsx

Name of Reagent/ Equipment	Company
2-0 silk suture	Ethicon
1/4" x 3/8" connector with luer	NovoSci
Masterflex platinum-cured silicone tubing	Cole-Parmer
infusion and outflow line	Smiths Medical
Polyester pouch (Ampak 400 Series SealPAK Pouches)	Fisher scientific
Snapware Square-Grip Canister	Snapware
Black rubber stoppers	VWR
Peristaltic pump	Harvard Apparatus
2 L aspirator bottle with bottom sidearm	VWR
Quant-iT PicoGreen dsDNA Assay kit	Life Technologies
Calf thymus standard	Sigma
Blyscan Glycosaminoglycan Assay Kit	Biocolor Ltd
Plate reader	Tecan
GE fluoroscopy	General Electric
Visipaque	GE

Catalog Number	Comments/Description
SA85H	Suture used to ligate superior and inferior vena cava
332023-000	Connect aorta and pulmonary artery
HV-96410-16	Tubing to connect heart chambers/veins
MX452FL	For flowing solutions through the vasculature
01-812-17	Pericardium-like pouch for containing heart during decellularization
1022	1-liter Container used for perfusing heart
59586-162	To seal the perfusion container
881003	To pump fluid through the inflow lines and to drain fluids
89001-532	For holding solutions/perfusate
P7589	For quantifying dsDNA
D4522	DNA standard
Blyscan #B1000	GAG assay kit
Infinite M200 Pro	For analytical assays
OEC 9900 Elite	Angiogram
13233575	Contrast agent

1 Alewife Center #200
Cambridge, MA 02140
tel. 617.945.9051
www.jove.com

ARTICLE AND VIDEO LICENSE AGREEMENT

Title of Article: Decellularization of whole human heart inside a pressurized pouch in an inverted orientation

Author(s): Doris A. Taylor, Luiz C. Sampaio, Rafael Cabello et al.

Item 1 (check one box): The Author elects to have the Materials be made available (as described at http://www.jove.com/author) via: [X] Standard Access [ ] Open Access

Item 2 (check one box):

[X] The Author is NOT a United States government employee.

[ ] The Author is a United States government employee and the Materials were prepared in the course of his or her duties as a United States government employee.

[ ] The Author is a United States government employee but the Materials were NOT prepared in the course of his or her duties as a United States government employee.

ARTICLE AND VIDEO LICENSE AGREEMENT

1. Defined Terms. As used in this Article and Video License Agreement, the following terms shall have the following meanings: "**Agreement**" means this Article and Video License Agreement; "**Article**" means the article specified on the last page of this Agreement, including any associated materials such as texts, figures, tables, artwork, abstracts, or summaries contained therein; "**Author**" means the author who is a signatory to this Agreement; "**Collective Work**" means a work, such as a periodical issue, anthology or encyclopedia, in which the Materials in their entirety in unmodified form, along with a number of other contributions, constituting separate and independent works in themselves, are assembled into a collective whole; "**CRC License**" means the Creative Commons Attribution-Non Commercial-No Derivs 3.0 Unported Agreement, the terms and conditions of which can be found at: http://creativecommons.org/licenses/by-nc-nd/3.0/legalcode; "**Derivative Work**" means a work based upon the Materials or upon the Materials and other pre-existing works, such as a translation, musical arrangement, dramatization, fictionalization, motion picture version, sound recording, art reproduction, abridgment, condensation, or any other form in which the Materials may be recast, transformed, or adapted; "**Institution**" means the institution, listed on the last page of this Agreement, by which the Author was employed at the time of the creation of the Materials; "**JoVE**" means MyJove Corporation, a Massachusetts corporation and the publisher of *The Journal of Visualized Experiments;* "**Materials**" means the Article and / or the Video; "**Parties**" means the Author and JoVE; "**Video**" means any video(s) made by the Author, alone or in conjunction with any other parties, or by JoVE or its affiliates or agents, individually or in collaboration with the Author or any other parties, incorporating all or any portion of the Article, and in which the Author may or may not appear.

2. Background. The Author, who is the author of the Article, in order to ensure the dissemination and protection of the Article, desires to have the JoVE publish the Article and create and transmit videos based on the Article. In furtherance of such goals, the Parties desire to memorialize in this Agreement the respective rights of each Party in and to the Article and the Video.

3. Grant of Rights in Article. In consideration of JoVE agreeing to publish the Article, the Author hereby grants to JoVE, subject to **Sections 4** and **7** below, the exclusive, royalty-free, perpetual (for the full term of copyright in the Article, including any extensions thereto) license (a) to publish, reproduce, distribute, display and store the Article in all forms, formats and media whether now known or hereafter developed (including without limitation in print, digital and electronic form) throughout the world, (b) to translate the Article into other languages, create adaptations, summaries or extracts of the Article or other Derivative Works (including, without limitation, the Video) or Collective Works based on all or any portion of the Article and exercise all of the rights set forth in (a) above in such translations, adaptations, summaries, extracts, Derivative Works or Collective Works and (c) to license others to do any or all of the above. The foregoing rights may be exercised in all media and formats, whether now known or hereafter devised, and include the right to make such modifications as are technically necessary to exercise the rights in other media and formats. If the "Open Access" box has been checked in **Item 1** above, JoVE and the Author hereby grant to the public all such rights in the Article as provided in, but subject to all limitations and requirements set forth in, the CRC License.

4. Retention of Rights in Article. Notwithstanding the exclusive license granted to JoVE in **Section 3** above, the Author shall, with respect to the Article, retain the non-exclusive right to use all or part of the Article for the non-commercial purpose of giving lectures, presentations or teaching classes, and to post a copy of the Article on the Institution's website or the Author's personal website, in each case provided that a link to the Article on the JoVE website is provided and notice of JoVE's copyright in the Article is included. All non-copyright intellectual property rights in and to the Article, such as patent rights, shall remain with the Author.

5. Grant of Rights in Video – Standard Access. This **Section 5** applies if the "Standard Access" box has been checked in **Item 1** above or if no box has been checked in **Item 1** above. In consideration of JoVE agreeing to produce, display or otherwise assist with the Video, the Author hereby acknowledges and agrees that, Subject to **Section 7** below, JoVE is and shall be the sole and exclusive owner of all rights of any nature, including, without limitation, all copyrights, in and to the Video. To the extent that, by law, the Author is deemed, now or at any time in the future, to have any rights of any nature in or to the Video, the Author hereby disclaims all such rights and transfers all such rights to JoVE.

6. Grant of Rights in Video – Open Access. This **Section 6** applies only if the "Open Access" box has been checked in **Item 1** above. In consideration of JoVE agreeing to produce, display or otherwise assist with the Video, the Author hereby grants to JoVE, subject to **Section 7** below, the exclusive, royalty-free, perpetual (for the full term of copyright in the Article, including any extensions thereto) license (a) to publish, reproduce, distribute, display and store the Video in all forms, formats and media whether now known or hereafter developed (including without limitation in print, digital and electronic form) throughout the world, (b) to translate the Video into other languages, create adaptations, summaries or extracts of the Video or other Derivative Works or Collective Works based on all or any portion of the Video and exercise all of the rights set forth in (a) above in such translations, adaptations, summaries, extracts, Derivative Works or Collective Works and (c) to license others to do any or all of the above. The foregoing rights may be exercised in all media and formats, whether now known or hereafter devised, and include the right to make such modifications as are technically necessary to exercise the rights in other media and formats. For any Video to which this Section 6 is applicable, JoVE and the Author hereby grant to the public all such rights in the Video as provided in, but subject to all limitations and requirements set forth in, the CRC License.

7. Government Employees. If the Author is a United States government employee and the Article was prepared in the course of his or her duties as a United States government employee, as indicated in **Item 2** above, and any of the licenses or grants granted by the Author hereunder exceed the scope of the 17 U.S.C. 403, then the rights granted hereunder shall be limited to the maximum rights permitted under such statute. In such case, all provisions contained herein that are not in conflict with such statute shall remain in full force and effect, and all provisions contained herein that do so conflict shall be deemed to be amended so as to provide to JoVE the maximum rights permissible within such statute.

8. Likeness, Privacy, Personality. The Author hereby grants JoVE the right to use the Author's name, voice, likeness, picture, photograph, image, biography and performance in any way, commercial or otherwise, in connection with the Materials and the sale, promotion and distribution thereof. The Author hereby waives any and all rights he or she may have, relating to his or her appearance in the Video or otherwise relating to the Materials, under all applicable privacy, likeness, personality or similar laws.

9. Author Warranties. The Author represents and warrants that the Article is original, that it has not been published, that the copyright interest is owned by the Author (or, if more than one author is listed at the beginning of this Agreement, by such authors collectively) and has not been assigned, licensed, or otherwise transferred to any other party. The Author represents and warrants that the author(s) listed at the top of this Agreement are the only authors of the Materials. If more than one author is listed at the top of this Agreement and if any such author has not entered into a separate Article and Video License Agreement with JoVE relating to the Materials, the Author represents and warrants that the Author has been authorized by each of the other such authors to execute this Agreement on his or her behalf and to bind him or her with respect to the terms of this Agreement as if each of them had been a party hereto as an Author. The Author warrants that the use, reproduction, distribution, public or private performance or display, and/or modification of all or any portion of the Materials does not and will not violate, infringe and/or misappropriate the patent, trademark, intellectual property or other rights of any third party. The Author represents and warrants that it has and will continue to comply with all government, institutional and other regulations, including, without limitation all institutional, laboratory, hospital, ethical, human and animal treatment, privacy, and all other rules, regulations, laws, procedures or guidelines, applicable to the Materials, and that all research involving human and animal subjects has been approved by the Author's relevant institutional review board.

10. JoVE Discretion. If the Author requests the assistance of JoVE in producing the Video in the Author's facility, the Author shall ensure that the presence of JoVE employees, agents or independent contractors is in accordance with the relevant regulations of the Author's institution. If more than one author is listed at the beginning of this Agreement, JoVE may, in its sole discretion, elect not take any action with respect to the Article until such time as it has received complete, executed Article and Video License Agreements from each such author. JoVE reserves the right, in its absolute and sole discretion and without giving any reason therefore, to accept or decline any work submitted to JoVE. JoVE and its employees, agents and independent contractors shall have

full, unfettered access to the facilities of the Author or of the Author's institution as necessary to make the Video, whether actually published or not. JoVE has sole discretion as to the method of making and publishing the Materials, including, without limitation, to all decisions regarding editing, lighting, filming, timing of publication, if any, length, quality, content and the like.

11. Indemnification. The Author agrees to indemnify JoVE and/or its successors and assigns from and against any and all claims, costs, and expenses, including attorney's fees, arising out of any breach of any warranty or other representations contained herein. The Author further agrees to indemnify and hold harmless JoVE from and against any and all claims, costs, and expenses, including attorney's fees, resulting from the breach by the Author of any representation or warranty contained herein or from allegations or instances of violation of intellectual property rights, damage to the Author's or the Author's institution's facilities, fraud, libel, defamation, research, equipment, experiments, property damage, personal injury, violations of institutional, laboratory, hospital, ethical, human and animal treatment, privacy or other rules, regulations, laws, procedures or guidelines, liabilities and other losses or damages related in any way to the submission of work to JoVE, making of videos by JoVE, or publication in *JoVE* or elsewhere by JoVE. The Author shall be responsible for, and shall hold JoVE harmless from, damages caused by lack of sterilization, lack of cleanliness or by contamination due to the making of a video by JoVE its employees, agents or independent contractors. All sterilization, cleanliness or decontamination procedures shall be solely the responsibility of the Author and shall be undertaken at the Author's expense. All indemnifications provided herein shall include JoVE's attorney's fees and costs related to said losses or damages. Such indemnification and holding harmless shall include such losses or damages incurred by, or in connection with, acts or omissions of JoVE, its employees, agents or independent contractors.

12. Fees. To cover the cost incurred for publication, JoVE must receive payment before production and publication the Materials. Payment is due in 21 days of invoice. Should the Materials not be published due to an editorial or production decision, these funds will be returned to the Author. Withdrawal by the Author of any submitted Materials after final peer review approval will result in a US$1,200 fee to cover pre-production expenses incurred by JoVE. If payment is not received by the completion of filming, production and publication of the Materials will be suspended until payment is received.

13. Transfer, Governing Law. This Agreement may be assigned by JoVE and shall inure to the benefits of any of JoVE's successors and assignees. This Agreement shall be governed and construed by the internal laws of the Commonwealth of Massachusetts without giving effect to any conflict of law provision thereunder. This Agreement may be executed in counterparts, each of which shall be deemed an original, but all of which together shall be deemed to me one and the same agreement. A signed copy of this Agreement delivered by facsimile, e-mail or other means of electronic transmission shall be deemed to have the same legal effect as delivery of an original signed copy of this Agreement.

A signed copy of this document must be sent with all new submissions. Only one Agreement required per submission.

CORRESPONDING AUTHOR:

Name:	Doris A. Taylor, PhD, FAHA, FACC
Department:	Regenerative Medicine Laboratory
Institution:	Texas Heart Institute
Article Title:	Decellularization of whole human heart inside a pressurized pouch in an inverted orientation
Signature:	 Date: 3/7/18

Please submit a signed and dated copy of this license by one of the following three methods:

1) Upload a scanned copy of the document as a pfd on the JoVE submission site;
2) Fax the document to +1.866.381.2236;
3) Mail the document to JoVE / Attn: JoVE Editorial / 1 Alewife Center #200 / Cambridge, MA 02139

For questions, please email submissions@jove.com or call +1.617.945.9051

TEXAS HEART® INSTITUTE

Doris Taylor, PhD, FAHA, FACC
Director, Regenerative Medicine Research
Co-Director, Biorepository and Sample Profiling Core, National Heart, Lung, and Blood Institute (NHLBI)
Cardiovascular Cell Therapy Research Network (CCTRN)
Director, Biorepository and Sample Profiling Core, Cardiothoracic Surgical Trials Network (CTSN)
Director, Center for Cell and Organ Biotechnology
Adjunct Professor, Department of Veterinary Physiology & Pharmacology, Texas A&M University
Adjunct Professor, Rice University Department of Biosciences

June 25, 2018

Phillip Steindel, Ph.D.
Review Editor
JoVE

Ref.: JoVE58123 Decellularization of Whole Human Heart inside a Pressurized Pouch in an Inverted Orientation

Dear Dr. Steindel:

Thank you for the editorial feedback. We have edited the manuscript based on the feedback.

Specific responses to the editorial comments are listed below:

Editorial comments:

1. Unfortunately, there are a few sections of the manuscript that show significant overlap with previously published work. Though there may be a limited number of ways to describe a technique, please use original language throughout the manuscript. Please see the attached iThenticate report, in particular lines: 212-217, 222-224, 231-235.

Response: *We have revised the manuscript to remove overlap with our previously published work. Many of the overlap, however, are names and concentrations of chemicals, solutions or sequence of steps that cannot be altered. Nevertheless, we have restructured these sentences to minimize overlap with our previous publications.*

2. Protocol: With formatting according to JoVE standards (spacing between all steps/substeps, all text aligned to the left margin; see attached revision), the protocol exceeds the maximum length for filming. Please highlight the portion of the protocol you wish to have filmed.

Response: *We have highlighted part (sections 1.4 to 2.3) of the protocol that we want to be filmed.*

3. Protocol: Please ensure that every step/substep has at least one action written in the imperative, and that each one contains no more than 2-3 actions or 4 sentences.

Response: *We have revised the protocol so that all steps/substeps now contain at least one action written in the imperative, and 2-3 actions or 4 sentences.*

4. Protocol 3: Can you comment on when exactly you might do these evaluations? For every heart?

Response: *We have added the clarification that the evaluations are performed in representative hearts.*

5. Table 1: Please remove from the manuscript and upload as a .xls/.xlsx file.

Response: *We have made Table 1 a separate excel file.*

6. Figure 6: '@ SDS 4d', not '@SDS d'.

Response: *We have corrected this error in Fig. 6.*

7. Figure 10: What should a cell look like here and what types of cells are shown? Also, it should be '50 μm' on the scale bar, not '50um'.

Response: *We have added arrows to indicate cells in the cadaveric tissue in Figure 10. We have also added that these cells are either cardiomyocytes or cardiac fibroblasts in the figure legend. We have changed the scale bar to be '50 μm'.*

8. Per your reply to Reviewer 3, could you comment a bit more in the manuscript about recellularization/the immune response as well as the residual coloring in Figure 6?

Response: *We have added a discussion on the recellularization/ immune response to the discussion section. This reads as: "A main goal for decellularized tissues is to be able to repopulate them with cells and achieve high cell attachment, proliferation, maturation and functionality. Our decellularized tissues have been successfully recellularized for various applications, where the tissues were successfully recellularized and achieved lower thrombogenicity."*

We now discuss the residual coloring in Figure 6 legend. This reads as: "The coloring in the human hearts is caused by residual lipofucin deposition. The coloring normally presents in inner ventricular surface or the boundary between epicardium and myocardium. "

Sincerely,

Doris A. Taylor, Ph.D., Hon D.Sc., FAHA, FACC
MC 2-255, PO Box 20345, Houston, TX 77225-0345, USA
Phone: 832-355-9481; Email: dataylor@texasheart.org